

## **Functional 1,3a,6a-triazapentalene scaffold: Design of fluorescent probes for kinesin spindle protein (KSP)**

Jun-ichi Sawada<sup>a,†</sup>, Ayumi Osawa<sup>b,c,†</sup>, Tomoki Takeuchi<sup>d</sup>, Masato Kaneda<sup>d</sup>, Shinya Oishi<sup>d,\*</sup>, Nobutaka Fujii<sup>d</sup>, Akira Asai<sup>a,\*</sup>, Keiji Tanino<sup>e</sup>, Kosuke Namba<sup>b,e</sup>

<sup>a</sup>Graduate School of Pharmaceutical Sciences, University of Shizuoka, Suruga-ku, Shizuoka 422-8526, Japan

<sup>b</sup>Graduate School of Pharmaceutical Sciences, The University of Tokushima, Tokushima 770-8505, Japan.

<sup>c</sup>Graduate School of Chemical Sciences and Engineering, Hokkaido University, Kita-ku, Sapporo 060-0810, Japan

<sup>d</sup>Graduate School of Pharmaceutical Sciences, Kyoto University, Sakyo-ku, Kyoto 606-8501, Japan

<sup>e</sup>Department of Chemistry, Faculty of Science, Hokkaido University, Kita-ku, Sapporo 060-0810, Japan

† Authors have made an equal contribution.

### **Corresponding Authors:**

Shinya Oishi, Ph.D.

Graduate School of Pharmaceutical Sciences

Kyoto University

Sakyo-ku, Kyoto 606-8501, Japan

Tel: +81-75-753-4561; Fax: +81-75-753-4570

E-mail: [soishi@pharm.kyoto-u.ac.jp](mailto:soishi@pharm.kyoto-u.ac.jp)

Akira Asai, Ph.D.

Graduate School of Pharmaceutical Sciences

University of Shizuoka

Shizuoka 422-8526, Japan

Tel: +81-54-264-5231; Fax: +81-54-264-5231

E-mail: [aasai@u-shizuoka-ken.ac.jp](mailto:aasai@u-shizuoka-ken.ac.jp)

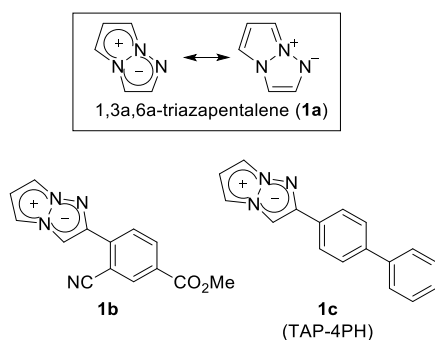
## Abstract

1,3a,6a-Triazapentalene is a compact fluorescent chromophore. In this study, triazapentalene was used to modify a series of biphenyl-type inhibitors of kinesin spindle protein (KSP) to develop fluorescent probes for the intracellular visualization of this protein. Microscopic studies demonstrated that these novel triazapentalene-labeled compounds exhibited inhibitory activity towards KSP in cultured cells and provided important information concerning the intracellular distribution.

**Keywords:** kinesin spindle protein; KSP; probe; triazapentalene

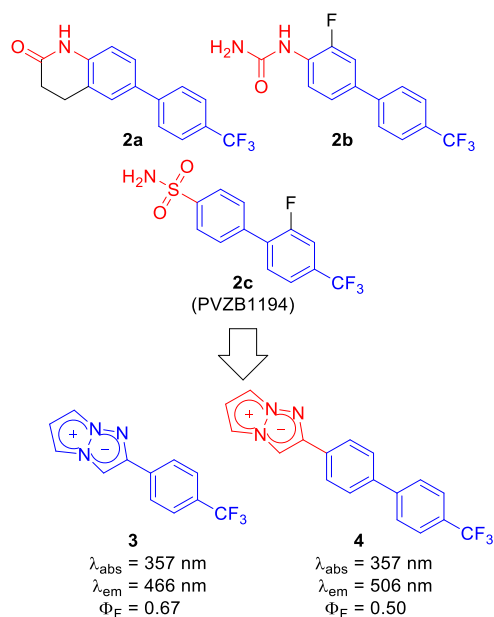
1,3a,6a-Triazapentalene **1** is a fluorescent chromophore with a high quantum yield (Figure 1).<sup>1</sup> This simple bicyclic heterocycle has been used to develop a variety of fluorescent dyes by the modification of its core structure at its 2-, 4- and 5-positions with a variety of different groups.<sup>2</sup> Cai's group reported the use of a gold-catalyzed triazole-alkyne cyclization to give a series of 1,3a,6a-triazapentalene derivatives.<sup>3</sup> To date, two triazapentalene derivatives have been employed to investigate changes in the morphological characteristics of cells.<sup>2b,4</sup> 2-[2-Cyano-4-(methoxycarbonyl)phenyl]triazapentalene **1b** was the first fluorescent probe to be shown to accumulate in the cytoplasm.<sup>2b</sup> 2-(Biphenyl-4-yl)triazapentalene **1c**, which is also known as TAP-4PH, has been used as a fluorescence imaging probe to visualize neuronal and neutrophilic differentiation processes in PC-12 and HL-60 cells, respectively.<sup>4</sup> We envisaged that this unique triazapentalene structure could be used as a pharmacophore functional group and incorporated into the aromatic heterocyclic scaffolds of novel drug candidates in medicinal chemistry to visualize their targets. The modification of the core structures of biomolecules and bioactive substances with this tiny triazapentalene scaffold could be used as a general strategy to allow for the fluorescent labeling of these compounds without any discernible loss in their original bioactivity. This approach would therefore provide favorable fluorescent probes for visualizing the distribution of bioactive substances, as well as the distribution of their target molecules in *in vitro* and *in vivo* experiments.<sup>5</sup>

**Figure 1.** Structures of 1,3a,6a-triazapentalene **1a** and the application of this group to the development of fluorescent probes **1b** and **1c** for probing morphological changes in cells.



Several research groups, including our own, have recently reported the development of kinesin spindle protein (KSP) inhibitors with potent antiproliferative activities (Figure 2). For example, substituted biphenyl derivatives **2** are unique KSP inhibitors. Notably, these compounds have been reported to exhibit potent activity against mutant KSP proteins, which are resistant to the allosteric KSP inhibitor, ispinesib.<sup>6</sup> Several 2,3-fused indole structures, including carbazoles and  $\beta$ -carboline, which are often observed in cytotoxic natural products, have been reported as effective alternatives to the traditional scaffolds described above for the preparation of KSP inhibitors.<sup>7</sup> Carbazole derivatives bearing different substituents at specific positions on their ring exhibited highly potent inhibitory activity towards KSP, as well as cytotoxicity towards human cancer cells.<sup>8</sup> Diarylamine-type inhibitors of KSP have also been designed to improve the aqueous solubility of fused indole-type KSP inhibitors.<sup>9</sup> The modification of these structures with a nonplanar cyclic moiety or a charged heterocyclic system afforded a novel series of potent KSP inhibitors with favorable physicochemical properties.<sup>10</sup> These molecules bearing simple aromatic scaffolds inhibited the microtubule-activated ATPase activity of the motor domain of KSP in an apparent ATP-competitive manner.

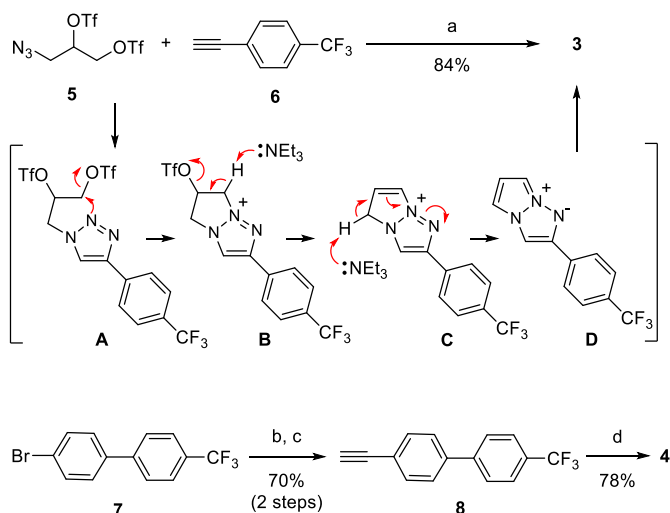
**Figure 2.** Design of novel KSP probes based on the structures of fluorescent 1,3a,6a-triazapentalene scaffold and biaryl-type KSP inhibitors.



KSP inhibitors inhibit the mitotic progression of the cell cycle, resulting in the accumulation of mitotic cells by suppressing the movement of centrosomes, which is required for the formation of bipolar spindles during early mitosis.<sup>11</sup> The results of phenotypic studies involving mitotic cells arrested by biphenyl-type inhibitors demonstrated that the monoastrol phenotype appeared to be similar to that achieved using allosteric inhibitors such as monastrol and *S*-trityl-cysteine (STLC). However, the intracellular distribution patterns of KSP as well as the binding sites on KSP were completely different in these two cases.<sup>6c,6d</sup> In addition, considerable differences were observed in the *in vitro* biochemical activities of biphenyl-type KSP inhibitors and their activities in cultured cell assays, which were supported by our structure-activity relationship studies.<sup>6c</sup> Indeed, some of biphenyl derivatives inhibited the proliferation of cells without causing cell cycle arrest at the mitosis stage, even though they showed good inhibitory activity against the ATPase activity of KSP *in vitro*. In this study, we have investigated the intracellular distribution of a biphenyl-type KSP inhibitor using a novel fluorescent probe. This study represents the first reported application of a 1,3a,6a-triazapentalene moiety as a bifunctional substructure with fluorescent and pharmacophoric properties for the visualization of bioactive substances and their targets.

The modification of a small molecule with a fluorescent probe or some other functional group often prevents the binding of the small molecule to the target molecule(s), leading to changes in the localization of the compound. To minimize the possibility of introducing an interactive functional group that could interfere with the biological activity of the parent molecule, we designed two different KSP inhibitors **3** and **4**. In these cases, a fluorescent 1,3a,6a-triazapentalene moiety was used as a phenyl surrogate and/or a terminal pharmacophore group to give two fluorescently-labeled biphenyl-type KSP inhibitors (Figure 2). Compounds **3** and **4** were synthesized according to our previously reported procedures (Scheme 1).<sup>1</sup> Briefly, alkyne **6** was directly converted to the target 4-(trifluoromethyl)phenyl derivative **3** via the formation of the Huisgen cycloaddition product **A**, followed by an aromatization process. The biphenyl-type congener **4** was obtained in a similar manner from alkyne **8**, which was prepared by the Sonogashira coupling of **7** with TMS-acetylene followed by the removal of the TMS protecting group.

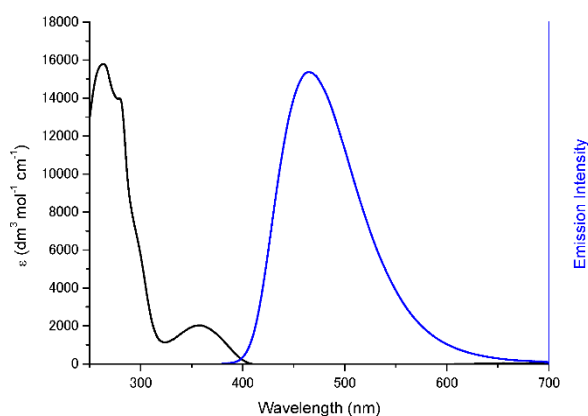
**Scheme 1.** Synthesis of the novel fluorescent KSP probes **3** and **4** bearing a 1,3a,6a-triazapentalene scaffold. *Reagents and conditions:* (a) CuI (5 mol %), (Me<sub>2</sub>NCH<sub>2</sub>CH<sub>2</sub>)<sub>2</sub>O (5 mol %), Et<sub>3</sub>N (5 equiv), THF (0.01 M), rt; (b) Trimethylsilylacetylene, CuI, Pd(PPh<sub>3</sub>)<sub>4</sub>, Et<sub>2</sub>N, DMF, 80 °C; (c) TBAF, THF, rt; (d) **5**, CuI (5 mol %), (Me<sub>2</sub>NCH<sub>2</sub>CH<sub>2</sub>)<sub>2</sub>O (5 mol %), Et<sub>3</sub>N (5 equiv), THF (0.01 M), rt.



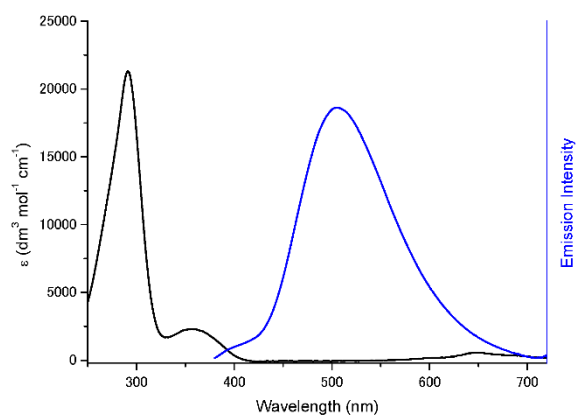
With the two triazapentalene derivatives (**3** and **4**) in hand, we proceeded to investigate their fluorescence properties in dichloromethane (Figure 3). The absorption spectra of compounds **3** and **4** contained characteristic absorption bands from 300 to 400 nm, with absorption maxima ( $\lambda_{\text{abs}}$ ) at 357 nm. The emission wavelengths ( $\lambda_{\text{em}}$ ) of compounds **3** and **4** were determined to be 466 and 506 nm, respectively, making them suitable for fluorescence microscopy analysis in cellular systems. These compounds also exhibited large Stokes shifts and high fluorescence quantum yields ( $\Phi_{\text{F}}$ ), which are favorable for excluding background signals.

**Figure 3.** The fluorescence spectra of the KSP probes in dichloromethane.

#### Compound 3

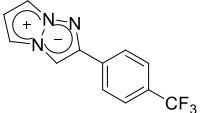
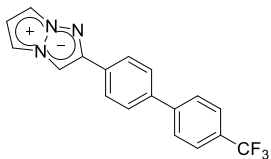


#### Compound 4



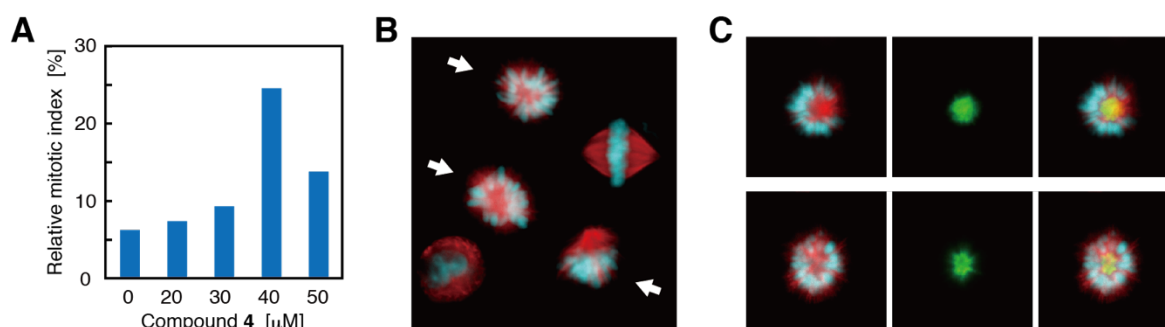
The inhibitory activities of compounds **3** and **4** against the microtubule-activated ATPase activity of KSP were determined using an *in vitro* ATPase assay. Compound **3** moderately inhibited the ATPase activity (34% inhibition at 20  $\mu$ M). Compound **4** gave an IC<sub>50</sub> value of 6.8  $\mu$ M (Table 1), which suggested that the introduction of a fluorescent triazapentalene moiety in **4** had a modest impact on the inhibitory activities of the parent compounds. Compounds **3** and **4** were subsequently examined for their anti-proliferative activity in HeLa human cervical adenocarcinoma cells and A549 lung adenocarcinoma cells using a growth inhibition assay. Compounds **3** and **4** gave GI<sub>50</sub> values of 25 and 19  $\mu$ M in HeLa cells, respectively (Table 1). In terms of their activity against A549 cells, compound **3** was much less potent than **4** [GI<sub>50</sub>(**4**) = 22  $\mu$ M]. These results suggested that both of these compounds were less potent than the parent inhibitor PVZB1194 (**2c**).<sup>6c</sup> Compound **4** was determined to be the most potent of the two compounds prepared in this study and was therefore selected for further evaluation in cells. To determine whether compound **4** could inhibit mitotic progression in cultured cells, we added it to synchronized HeLa cells as they entered the M phase of the cell cycle. The cells were then cultured for 4 h at 37 °C before being fixed and visualized by immunofluorescence. Microscopic observations revealed that there was a concentration-dependent accumulation of mitotic cells, with a concentration of 40  $\mu$ M of **4** being particularly effective for inhibiting the division of these cells (Figure 4A). The reduction in mitotic index at 50  $\mu$ M of **4** resulted from its poor solubility in the medium, as microscopic observations found the deposition of insoluble **4** at concentrations above 50  $\mu$ M. The narrow window for the effective concentrations was attributed to the poor solubility and the moderate inhibitory activity of compound **4** against the ATPase activity of KSP. The major phenotype of the cells arrested in the M phase by 40  $\mu$ M of **4** was prometaphase with monopolar spindles (63% of the mitotic cells), which is consistent with the phenotype induced by KSP inhibitors (Figure 4B).<sup>6c</sup> The KSP inhibitory activity of **4** was also supported by the unique and irregular accumulation of KSP in the central region of the mitotic cells, which is consistent with the intracellular localization induced by other biphenyl-type KSP inhibitors (Figure 4C).<sup>6c</sup> These results therefore indicated that compound **4** could bind to KSP and inhibit its activity in cultured cells.

**Table 1.** KSP inhibitory activities and inhibitory effects on cell proliferation of fluorescent KSP probes.

compound	KSP ATPase IC <sub>50</sub> (μM) <sup>a,b</sup>	HeLa cells GI <sub>50</sub> (μM) <sup>c</sup>	A549 cells GI <sub>50</sub> (μM) <sup>c</sup>	
	<b>3</b>	>20 <sup>d</sup>	25 ± 0.7	>30 <sup>e</sup>
	<b>4</b>	6.8 ± 2.8	19 ± 0.5	22 ± 5.8

<sup>a</sup>Inhibition of microtubule-activated ATPase activity of KSP. <sup>b</sup>IC<sub>50</sub> values were calculated from three independent experiments. <sup>c</sup>The data were obtained from at least three independent experiments by the MTS assay. <sup>d</sup>34% inhibition at 20 μM. <sup>e</sup>6% cell growth inhibition at 30 μM.

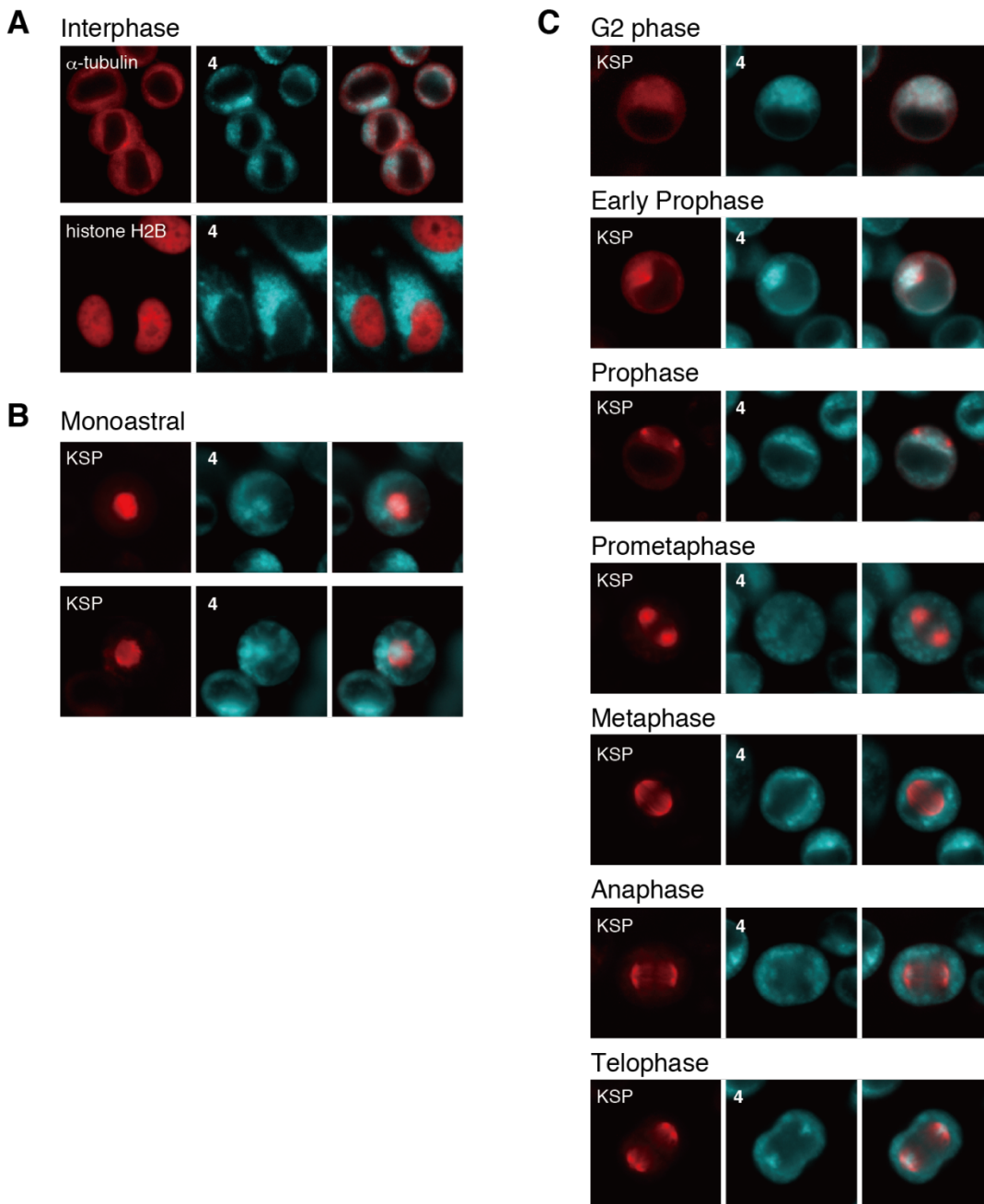
**Figure 4.** Potential KSP inhibitory activity of compound **4** in cultured cells. (A) Compound **4** attenuated the mitotic progression of HeLa cells in a concentration-dependent manner. The average relative mitotic indices of two independent experiments are shown (see Supplementary experimental procedure). (B and C) Fluorescent microscopy images of HeLa cells treated with 40 μM of **4**. After incubating synchronized cells with **4** for 4 h, the cells were fixed and immunostained. The arrows in (B) indicate the prometaphase cells with monopolar spindles. Two representative examples of the monoastral mitotic cells are shown in (C). Red, cyan and green signals were obtained using an anti-α-tubulin antibody, DAPI (4',6-diamidino-2-phenylindole) and an anti-KSP antibody, which showed microtubules, chromosomes and KSP, respectively. The right panels in (C) show the merged images of these colors. Notably, compound **4** was washed out during the immunostaining procedure.



HeLa cells expressing  $\alpha$ -tubulin or histone H2B, which were conjugated with hmAG1 fluorescent proteins as organelle specific markers of the cytoplasm and nucleus, respectively, were used to investigate the intracellular distribution of compound **4**.<sup>12</sup> The cells were incubated with **4** for 20 min at 37 °C to prior to visualizing its localization. Live cell imaging using fluorescent microscopy showed that compound **4** gave a much stronger fluorescent signal inside the cells than it did outside the cells (Figure 5A). This efficient uptake of **4** into the cells suggested that the triazapentalene fluorophore had not had an adverse impact on the membrane permeability of this compound. The fluorescent signals of **4** were mainly localized in the cytoplasm of the interphase cells, where KSP localizes during the interphase, rather than in the nucleus.<sup>11</sup>

To further determine the intracellular destination of **4**, we used HeLa cells stably expressing KSP conjugated to a hmAG1 fluorescent protein at its N-terminus. This fluorescent KSP recombinant protein localized in the same way as the endogenous protein through mitosis and cytokinesis without affecting the cell cycle process (Figure 5C).<sup>11</sup> Compound **4** (40  $\mu$ M) was incubated with mitotic cells for 20 min at 37 °C to visualize its localization. In the monoastral mitotic cells induced by compound **4**, some of the fluorescence associated with this compound overlapped with the central localization of KSP (Figure 5B). In contrast, as it was in the cells treated with 20  $\mu$ M of **4**, we did not observe any inhibition of mitosis in these cells, and the fluorescence of **4** did not accumulate where KSP localized through the mitotic phases (Figure 4A and 5C). However, the fluorescence of **4** appeared to overlap well with the localization of KSP in the G2 and early mitotic phases (Figure 5C). This result indicated that compound **4** would exhibit desirable localization properties in the situations where KSP was contributing to centrosomal movement to establish a bipolar structure during the early mitotic phases. These data therefore demonstrate that compound **4** labeled mitotic KSP with partial specificity in cultured cells. The sub-localization of **4** in the cellular region devoid of KSP suggests that possible unexpected side-effects of **4** could be attributed to alternative intracellular sites of action.<sup>13</sup>

**Figure 5.** Fluorescent microscopy images of HeLa cells stained with compound **4**. (A) HeLa cells expressing fluorescent  $\alpha$ -tubulin or fluorescent histone H2B were treated with 20  $\mu$ M of probe **4** for 20 min. (B and C) Mitotic HeLa cells expressing fluorescent KSP were treated with 40  $\mu$ M (B) or 20  $\mu$ M (C) of probe **4** for 20 min. Fluorescent images of cells with the monoastral phenotype (B) and normal mitotic phases (C). Compound **4** and the fluorescent proteins are shown in cyan and red, respectively. The cells were classified into each mitotic phase by visual inspection to determine the localization of their intracellular KSP.



In summary, we have designed and synthesized two novel fluorescently-labeled KSP inhibitors **3** and **4** using a 1,3a,6a-triazapentalene scaffold. The dual pharmacophore and fluorophore functions of the 1,3a,6a-triazapentalene moiety did not have an adverse impact on the KSP inhibitory activities of the parent biphenyl-type inhibitors. Microscopic imaging studies revealed not only the intracellular distribution profile of **4**, but also the partial colocalization of **4** with KSP, suggesting that the biphenyl derivative **4** could potentially be used as a small-molecule fluorescent probe for KSP. Compound **4** was also observed in areas of the cell where there is no KSP, suggesting that there could be secondary target(s) for this biphenyl-type system, which could explain some of its side effects. Taken together, the results of this study provide a good example of the compatibility between the bioactivity and intracellular distribution of small-molecule inhibitors. Further studies towards the potential application of this 1,3a,6a-triazapentalene fluorophore for analyzing the mechanisms of action of different drugs and visualizing their target proteins are currently in progress in our laboratory.

### **Acknowledgments**

This work was supported by Grants-in-Aid for Scientific Research (23390025, 24310162, 26102734, 25-5388, 26-2457) from JSPS, Japan; Platform for Drug Discovery, Informatics, and Structural Life Science from MEXT, Japan. A.O., T.T. and M.K. are grateful for JSPS Research Fellowships for Young Scientists. K.N. is grateful to the Naito Foundation for support through a Research Fund for Recently Independent Professor.

### **Supplementary data**

Supplementary data (experimental procedures and spectral data) associated with this article can be found, in the online version, at #####.

## References and Notes

1. Namba, K.; Osawa, A.; Ishizaka, S.; Kitamura, N.; Tanino, K. *J. Am. Chem. Soc.* **2011**, *133*, 11466.
2. (a) Namba, K.; Mera, A.; Osawa, A.; Sakuda, E.; Kitamura, N.; Tanino, K. *Org. Lett.* **2012**, *14*, 5554. (b) Namba, K.; Osawa, A.; Nakayama, A.; Mera, A.; Tano, F.; Chuman, Y.; Sakuda, E.; Taketsugu, T.; Sakaguchi, K.; Kitamura, N.; Tanino, K. *Chem. Sci.* **2015**, *6*, 1083. (c) Nakayama, A.; Nishio, S.; Otani, A.; Mera, A.; Osawa, A.; Tanino, K.; Namba, K. *Chem. Pharm. Bull.* **2016**, *64*, 830.
3. Cai, R.; Wang, D.; Chen, Y.; Yan, W.; Geise, N. R.; Sharma, S.; Li, H.; Petersen, J. L.; Li, M.; Shi, X. *Chem. Commun.* **2014**, *50*, 7303.
4. Kamada, R.; Tano, F.; Kudoh, F.; Kimura, N.; Chuman, Y.; Osawa, A.; Namba, K.; Tanino, K.; Sakaguchi, K. *PLOS ONE*, **2016**, *11*, e0160625.
5. For recent reviews, see: (a) Terai, T.; Nagano, T. *Pflugers Arch.* **2013**, *465*, 347. (b) Li, X.; Gao, X.; Shi, W.; Ma, H. *Chem. Rev.* **2014**, *114*, 590. (c) Lavis, L. D.; Raines, R. T. *ACS Chem. Biol.* **2014**, *9*, 855.
6. (a) Parrish, C. A.; Adams, N. D.; Auger, K. R.; Burgess, J. L.; Carson, J. D.; Chaudhari, A. M.; Copeland, R. A.; Diamond, M. A.; Donatelli, C. A.; Duffy, K. J.; Faucette, L. F.; Finer, J. T.; Huffman, W. F.; Hugger, E. D.; Jackson, J. R.; Knight, S. D.; Luo, L.; Moore, M. L.; Newlander, K. A.; Ridgers, L. H.; Sakowicz, R.; Shaw, A. N.; Sung, C. M. M.; Sutton, D.; Wood, K. W.; Zhang, S. Y.; Zimmerman, M. N.; Dhanak, D. *J. Med. Chem.* **2007**, *50*, 4939. (b) Luo, L.; Parrish, C. A.; Nevins, N.; McNulty, D. E.; Chaudhari, A. M.; Carson, J. D.; Sudakin, V.; Shaw, A. N.; Lehr, R.; Zhao, H.; Sweitzer, S.; Lad, L.; Wood, K. W.; Sakowicz, R.; Annan, R. S.; Huang, P. S.; Jackson, J. R.; Dhanak, D.; Copeland, R. A.; Auger, K. R. *Nat. Chem. Biol.* **2007**, *3*, 722. (c) Matsuno, K.; Sawada, J.; Sugimoto, M.; Ogo, N.; Asai, A. *Bioorg. Med. Chem. Lett.* **2009**, *19*, 1058. (d) Yokoyama, H.; Sawada, J.; Katoh, S.; Matsuno, K.; Ogo, N.; Ishikawa, Y.; Hashimoto, H.; Fujii, S.; Asai, A. *ACS Chem. Biol.* **2015**, *10*, 1128.

7. (a) Dhanak, D.; Knight, S. D.; Moore, M. L.; Newlander, K. A. PCT Int. Appl. WO2006005063, 2006. (b) Oishi, S.; Watanabe, K.; Ito, S.; Tanaka, M.; Nishikawa, H.; Ohno, H.; Shimane, K.; Izumi, K.; Sakagami, Y.; Kodama, E. N.; Matsuoka, M.; Asai, A.; Fujii, N. *J. Med. Chem.* **2010**, *1*, 276.
8. Takeuchi, T.; Oishi, S.; Watanabe, T.; Ohno, H.; Sawada, J.; Matsuno, K.; Asai, A.; Asada, N.; Kitaura, K.; Fujii, N. *J. Med. Chem.* **2011**, *54*, 4839.
9. Takeuchi, T.; Oishi, S.; Kaneda, M.; Ohno, H.; Nakamura, S.; Nakanishi, I.; Yamane, M.; Sawada, J.; Asai, A.; Fujii, N. *ACS Med. Chem. Lett.* **2014**, *5*, 566.
10. Takeuchi, T.; Oishi, S.; Kaneda, M.; Misu, R.; Ohno, H.; Sawada, J.; Asai, A.; Nakamura, S.; Nakanishi, I.; Fujii, N. *Bioorg. Med. Chem.* **2014**, *22*, 3171.
11. Blangy, A.; Lane, H. A.; d'Herin, P.; Harper, M.; Kress, M.; Nigg, E. A. *Cell.* **1995**, *29*, 1159.
12. Kanda, T.; Sullivan, K. F.; Wahl, G. M. *Curr. Biol.* **1998**, *8*, 377.
13. The possibility of a small portion of the probe existing in the cytoplasm without binding to a specific target could not be ruled out. Compound **4** inhibited cell cycle progression of interphase as well as mitosis at high concentrations above 40  $\mu$ M.